

UDC 533.9

V. I. Karas`,
prof., KhNAME,
NSC KIPT of
NASU

V. I. Golota, PhD,
NSC KIPT of
NASU

A. M. Yegorov,
Corresponding
Member of
NASU, NSC
KIPT of NASU

I. F. Potapenko,
prof., KIAM of
RAS

A. G. Zagorodny,
Academician,
BITP of NASU

MICROWAVE RADIATION WITH STOCHASTICALLY JUMPING PHASE: GENERATION AND APPLICATION TO DEVELOP A NEW TYPE OF OPTICAL RADIATION SOURCES

1. Introduction. Extensive research has been devoted to the theoretical and experimental investigation of the interaction of charged particle beams with plasma.

This interest is due to the fact that the beam-plasma instability, predicted by A.I. Akhiezer and Ya.B. Fainberg [1-3], is one of the prevalent instabilities. It results from a resonance interaction of charged particles with the waves excited in plasma. This interaction may be used for such important applications as high-power beam-plasma generators (BPG); high-current plasma accelerators of electrons, protons, and multicharged ions; plasma heating to high temperatures, etc. [4, 5].

The main advantage of plasma-beam generators is their ability to excite unprecedented-power oscillations: as the electron beam propagates in plasma, its own electric and magnetic fields are compensated; as a result, the achievable electron beam power and, consequently, the achievable power of excited plasma oscillations, are substantially higher as compared to devices in which the electron beam propagates in vacuum.

Owing to the excitation of bulk waves (rather than the surface ones, as in vacuum microwave generators) the efficiency of interaction between the electron beams and the excited plasma waves is substantially enhanced. In addition, these waves may be excited in larger volumes.

The frequency of excited oscillations is mainly determined by plasma density, and does not depend on geometrical dimensions; thus, one can excite the waves in volumes with linear dimensions much larger than the wavelength.

The wavelength of generated oscillations can be varied over a wide range by changing the plasma density.

When an unmodulated high-power electron beam interacts with plasma, the reverse action of excited waves on the beam causes a beam electron velocity distribution spread. Simultaneously, the excited-wave frequency and phase velocity spectra are broadened. As a result of a nonlinear interaction, the waves become stochastic.

However, some applications require generators and amplifiers of regular oscillations. This poses the problem of control: one should be able to either stabilize and suppress the unwanted instabilities, or to excite the useful intense oscillations with predetermined frequency and phase velocity spectra, as well as, a present stochasticity degree. The results of our previous studies on controlling the characteristics of BPG-generated oscillations were published in [6, 7].

High-frequency (HF) heating is very important field in connection with fundamental questions of plasma physics and applications. This area of physics is intensively investigated as theoretically and experimentally (for example, see [8-17] and references therein). The issues widely discussed in literature are connected with additional plasma heating in tokamaks [8-11], the nature of accelerated particles in space plasmas [12, 13], gas discharge physics [14, 15]. Among the problems that attract attention of scientific community is development of sources with solar spectrum. This is utmost important problem from the point of fundamental, as well as practical application, and in this direction interesting achievements is obtained (see, for example [16, 17]). It is worth mentioning that one of the difficulties associated with additional plasma heating in tokamaks is a well-known dependence of the Rutherford cross-section on velocity. As a consequence, the probability of collisions decreases with plasma temperature rising, thus creating obstacles for further plasma heating. Another important challenge in interaction of HF radiation with plasma is a barrier of the radiation penetration into the overdense plasma. To our knowledge, the most part of investigations in this direction are made with help of HF generators of electromagnetic radiation with regular phase. Thus the new opportunities that microwave radiation with jumping phase provides in this area would be very important.

In this paper, we describe also the results of the theoretical and experimental investigation of the plasma interaction with microwave radiation with jumping phase that obtained with help of the unique beam-plasma generator (BPG) made in KIPT [18]. This study continues research on behaviour of plasma discharge subjected to microwave radiation with stochastically jumping phase (MWRSJP) which started in [19-21]. The paper is organized as follows. The first section contains introduction and brief review of previous research. In Section 2, it is considered the interaction of a tubular electron beam with the plasma of a so-called helix-plasma waveguide (HPW) being a plasma waveguide placed into a helix slow-wave structure. In order to clarify the relative contributions of plasma and helix to oscillation excitation and power output, we investigated the influence of the helix on the plasma waveguide dispersion properties. In Section 3, it is presented an experimental device layout that was used to study the generation conditions for quasi-cw stochastic oscillations in the decimeter wavelength band. This apparatus consisted of electron-optical and electrodynamic units, a collector, and a solenoid. In Section 4, in the BPG experimental studies it was measured the electron beam current and energy, working gas pressure, plasma density, power and frequency spectrum of generated microwave oscillations, and the microwave oscillation pulse envelopes. To determine the stochasticity degree of the generated oscillations it was used the realization method followed by Fourier-analysis of oscillations. There are computed the autocorrelation functions, the correlation times, and the integral and differential amplitude distributions. In Section 5, It is considered a comparizon the theoretical results with the experimental data on the collective interaction between the electron beam and the helix-plasma waveguide waves, it is, above all, determined the beam parameters and the plasma density. In section 6, there are considered the experimental parameters of MWRSJP obtained from the BPG. The scheme of measurement of various parameters is given and experimental studies of optical radiation from the plasma discharge initiated by

MWRSJP are presented. Concluding remarks follow at the end.

It was shown in [21–23], both theoretically and experimentally, that the phenomenon of anomalous penetration of microwave radiation into plasma, conditions for gas breakdown and maintenance of a microwave gas discharge, and collisionless electron heating in a microwave field are related to jumps of the phase of microwave radiation. In this case, in spite of the absence of pair collisions or synchronism between plasma particles and the propagating electromagnetic field, stochastic microwave fields exchange their energy with charged particles. In such fields, random phase jumps of microwave oscillations play the role of collisions and the average energy acquired by a particle over the field period is proportional to the frequency of phase jumps.

Gas breakdown and maintenance of a discharge in a rarefied gas by a pulsed MWRSJP were studied theoretically and experimentally in [22–26], as well as propagation of this radiation within the plasma produced in such a way. The conditions for ignition and maintenance of a microwave discharge in air by MWRSJP were found. The pressure range in which the power required for discharge ignition and its maintenance has its minimum was determined [24–26]. It was shown that, in the interval of pressures that have a level less than optimal (about 50 Pa for argon), the minimum of MWRSJP breakdown power depends weakly on the working gas pressure owing to several reasons. These reasons are efficient collisionless electron heating, weakening of diffusion and, finally, decrease of elastic and inelastic collisional losses. This allows one to extend the domain of discharge existence toward lower pressures. The intensity of collisionless electron heating increases with increasing rate of phase jumps in MWRSJP. There is an optimal phase jump rate at which the rate of gas ionization and, accordingly, the growth rate of the electron and ion densities reach their maximum. The optimal phase jump rate is equal to the ionization frequency at electron energies close to the ionization energy of the working gas.

In the present work, the effect of high power pulsed decimeter MWRSJP action on a plasma, produced in a coaxial waveguide filled with a rarefied gas, is investigated with use of the above mentioned BPG [18], which was upgraded for the given experimental conditions. The goal of this work is to study the special features of low pressure discharge initiated by MWRSJP and also optical radiation spectra. For interpretation of the experimental results on the ignition and maintenance of a microwave discharge in air obtained with MWRSJP BPG, a numerical code has been developed. This code allows simulating the process of gas ionization by electrons heated in the MWRSJP field and studying the behaviour of plasma particles in such a field.

2. Basic theory. In general, the BPG electron beam-plasma interaction zone consists of a waveguide structure (a waveguide or some slow-wave system) combined with a plasma waveguide. In this article it is considered the interaction of a tubular electron beam with the plasma of a so-called helix-plasma waveguide (HPW) being a plasma waveguide placed into a helix slow-wave structure. In order to clarify the relative contributions of plasma and helix to oscillation excitation and power output, we investigated the influence of the helix on the plasma waveguide dispersion properties.

The most interesting case occurs when there is such a high plasma density that some bulk waves in the plasma-occupied domain exhibit a slowing-down weakly dependent on the parameters of the helix. Assume now the simplest tubular model of plasma density radial distribution, which is representative of a wide class of density profiles and, at the same time, relatively simple to treat analytically.

To simplify the calculations replace the helix with an impedance cylinder of radius d . Consider the bulk waves of the tube-shaped $0 < a < r < b < d$ plasma coaxial with the impedance (outer) cylinder. One gets the following dispersion equation for these waves:

$$\frac{k_{\perp} a J_1(k_{\perp} a) + A_i J_0(k_{\perp} a)}{k_{\perp} b J_1(k_{\perp} b) + A_e J_0(k_{\perp} b)} = \frac{k_{\perp} a N_1(k_{\perp} a) + A_i N_0(k_{\perp} a)}{k_{\perp} b N_1(k_{\perp} b) + A_e N_0(k_{\perp} b)} \quad (1)$$

with the notation

$$A_i = \frac{\kappa a I_1(\kappa a)}{I_0(\kappa a)}, \quad A_e = \kappa b \frac{I_1(\kappa b) - R k_i(\kappa b)}{I_0(\kappa b) - R k_0(\kappa b)},$$

$$R = \frac{I_0(\kappa d) - I_1(\kappa d) \frac{k_0}{\kappa} Z_0}{k_0(\kappa d) - k_1(\kappa d) \frac{k_0}{\kappa} Z_0}, \quad \text{where } Z_0 \text{ is the cylinder}$$

impedance, $\kappa^2 = k_0^2 - k^2$, $k_{\perp} = nk$.

With $Z_0 \rightarrow 0$, $b \rightarrow d$, and $a \rightarrow 0$ relation (1) tends to the dispersion equation for a plasma cylinder with conducting liner. If the outer and inner tube radii a and b , respectively, are finite, this equation describes the dispersion of the annular plasma bulk waves inside the conducting liner. Denote the helix and plasma waveguide wave slowing-down factors by N_h and N_p , respectively. If $N_h \gg N_p$, the helix contribution to the plasma waveguide dispersion characteristics, is insignificant.

The phase velocity in the system is shown to decrease with the decrease of helix pitch, and to increase with the increase of plasma density.

The tubular waveguide dispersion equation (1) makes it possible to find the threshold plasma density, at which there exists a slow wave with phase velocity v_0 for a given frequency ω_0 [8, 9]. In the limit of small v_0 , when $\kappa a \gg 1$, this equation is substantially simplified and becomes:

$$\tan[\kappa n(b-a)] = \frac{n}{1+n^2}, \quad \text{where } n^2 = \frac{\omega_p^2}{\omega_0^2} - 1. \quad (2)$$

It follows from this equation that for a relatively small plasma tube thickness, when $\omega_0(b-a)/v_0 \ll 1$, the first eigenvalue of the transverse wavenumber $\lambda_1 = \kappa n(b-a)$ lies within the $0 < \lambda_1 < \pi/2$ range. The corresponding plasma refractive index $n_0 = \lambda_1 v_0 / \omega_0(b-a)$ increases with plasma thickness decrease. The critical plasma density is defined in this case by the formula [27, 28]:

$$n_{per}[\text{cm}^{-3}] = 10^{-8} \left[f_0^2 + \frac{\lambda_1^2 v_0^2}{4\pi^2 (b-a)^2} \right]. \quad (3)$$

Here f_0 is the operating frequency in Hz; a and b are radii in cm; the v_0 velocity is in cm/s.

In case of low beam currents, one can neglect any space-charge wave field-distribution change due to the beam. Then the total increment of oscillation build-up in the system is proportional to the beam current. This makes it possible to calculate the threshold beam current corresponding to the beginning of system self-excitation under the condition that this increment (with account of radiation losses) is equal to zero:

$$J_{th} = \frac{e\beta_0^2 f_0 \omega \sigma_b}{r_0 L Q \mu}, \quad (4)$$

where $\beta_0 = v_0/c$, r_0 is the electron classical radius; L , Q and σ_b represent the system length, the quality factor, and the beam cross section area, respectively.

The increase of beam current brings about a transition from the discrete spectrum of excited oscillations to a continuous one. This takes place at the critical current:

$$J_{cr} = J_{th} \left[1 + \frac{1}{\ln \frac{\cot \psi + 1}{\cot \psi - 1}} \right]. \quad (5)$$

The relation $\omega = k_{\parallel} v$ not only defines the frequency spectra of excited oscillations, but also allows one to point out possible spectrum broadening mechanisms.

One of these mechanisms involves the increase of beam particle velocity spread due to the beam interaction with a wave pertaining to the slow-wave structure.

If the slow-wave system can support the propagation of waves with $v_p = v_0 \pm \Delta v$ phase velocities, then the beam accelerated and decelerated particles will also radiate, but now they will radiate at frequencies

$$\omega = k_{0\parallel}(\omega)(v_0 \pm \Delta v).$$

The resulting spectrum broadening can be found from the equation $\omega = k_{\parallel} v$:

$$\Delta\omega = \frac{k_{0\parallel} \Delta v}{1 - v_{gr}/v_0} \ll \omega_0, \quad v_{gr} = \frac{\partial\omega}{\partial k_{\parallel}}, \quad (6)$$

$$k_{0\parallel}(\omega_0) = \omega_0 / v_0.$$

For the excited oscillations to be stochastic, the frequency interval between the adjacent harmonics must be small in comparison with the bandwidth of each excited harmonic.

3. Experimental laboratory device. Figure 1 presents an experimental device layout we used to study the generation conditions for quasi-cw stochastic oscillations in the decimeter wavelength band. This apparatus consisted of electron-optical and electrodynamic units, a collector, and a solenoid. In addition, there were working gas leak-in and pump-out systems. A working gas pressure gradient transit tube and an open resonator to measure the plasma electron density were placed between the electron-optical and electrodynamic units.

We employed a longitudinal magnetic field from 0.12 to 0.16 T to transport the beam. The beam-plasma interaction zone was inside the electrodynamic slow-wave system. The gas pressure in the interaction zone was about 10^{-4} - 10^{-5} Torr, and from 10^{-6} - 5×10^{-7} Torr in the electron gun region. In order to study the generation of high-power microwave oscillations in the decimeter wavelength band, we developed an experimental quasi-cw 100 kW power laboratory device with a pulse length of 200 μ s, (see diagram Fig. 1). In the upper part of this figure one sees the sectioned solenoid longitudinal magnetic field distribution.

The experimental laboratory setup consisted of an electron gun (1), a slow-wave structure (9) inside the shield (7), an electron collector (15) with a single Langmuir probe (13), microwave feeders (5) and (10), and a solenoid (8). The system to maintain and control the working gas pressure consisted of the vacuum lines (3) and (14), a pressure gradient tube (4), the working gas leak-in valves (6) and (11), and the pressure control gauges (2) and (12).

The electron gun cathode was fed with negative high-voltage (up to 20 kV) 200 μs pulses with a repetition rate from 1 to 10 s^{-1} ; the electron anode gun was grounded. The electron beam passed through the pressure gradient tube and the slow-wave structure. After that it was dumped to a collector. The slow-wave system was placed inside a metal screen, which simultaneously played the role of the apparatus housing. The plasma was created in the slow-wave structure.

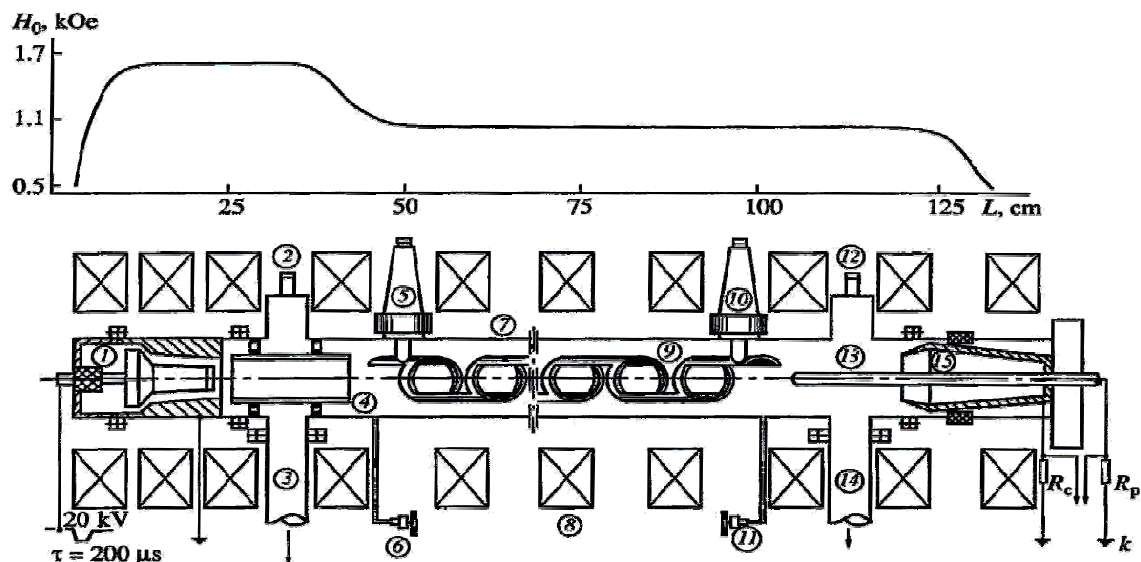


Fig. 1 – Experimental device layout and magnetic field distribution: (1) electron gun; (2) and (12) control pickups; (3) and (14) vacuum lines; (4) working gas pressure gradient tube; (5) and (10) high-frequency feeders; (6) and (11) working gas admission valves; (7) shielding screen; (8) solenoid; (9) slow-wave structure; (13) single Langmuir probe; (15) electron collector.

In this experimental laboratory apparatus we used a magnetron-type electron gun [10]. It was initiated via impact ionization of gas molecules by beam electrons. After that, a beam-plasma discharge (BPD) occurred, which produced a 3.0 cm o.d. and 2.2 cm i.d. tubular electron beam with an accelerating voltage of 20 kV and a current of 12 A.

A double modified helix [11] was chosen as a slow-wave structure. Its slowing-down coefficient, coupling impedance, and characteristic wave impedance are larger compared to the usual single helix structure. The helix slow-wave structure was designed for a beam synchronous velocity of 6.5×10^9 cm/s, which corresponds to a 13.2 keV beam electron energy. The helix geometrical parameters were as follows: 4.0 cm o.d., 3.6 cm i.d., 2.4 cm pitch, 0.6 cm ring width, 11 jumper half-angle, 46.0 cm length, and 6.6 cm shielding screen diameter.

The cold measurements of the dispersion characteristics showed that this modified double helix structure had a normal positive dispersion in the frequency range from 0.5 to 1.66 GHz. To obtain the required slowing-down coefficient value we varied both the jumper angle and the helix pitch at a fixed electron beam diameter. The slowing-down coefficient $n = c/v_0$ is enhanced with increasing jumper angle and helix pitch.

4. Experimental results. Measurement of beam, plasma, and microwave oscillation parameters.

In the BPG experimental studies we measured the electron beam current and energy, working gas pressure, plasma density, power and frequency spectrum of generated microwave oscillations, and the microwave oscillation pulse envelopes.

To determine the stochasticity degree of the generated oscillations we used the

realization method followed by Fourier-analysis of oscillations. We computed the autocorrelation functions, the correlation times, and the integral and differential amplitude distributions. The phase-frequency analysis of oscillations [12-14] provided data on their frequency, phase, and amplitude

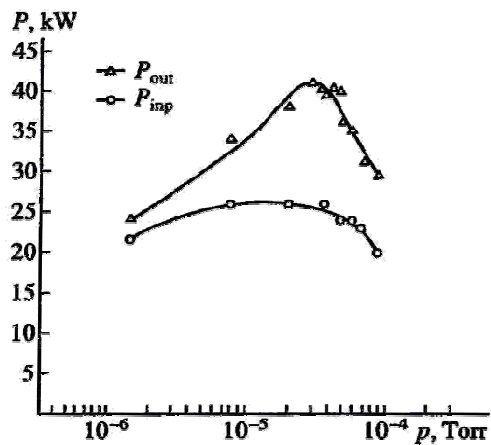


Fig. 2 – Pulse power vs. working gas pressure

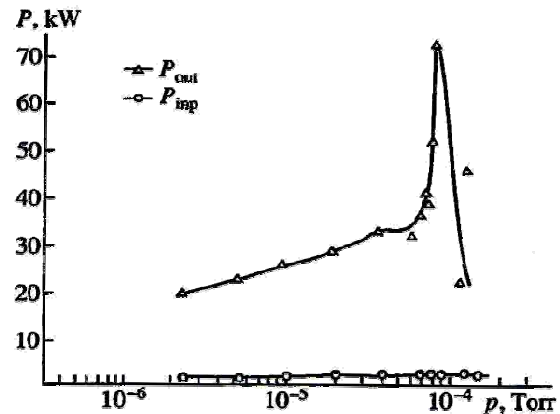


Fig. 3 – Pulse power vs. working gas pressure

A 19 keV energy, 9 A current, and 200 μ s pulse duration electron beam passed through the gas pressure gradient tube and open resonator, entered the interaction region, and was dumped at the collector.

In this experiment we investigated the excited oscillation power at the entrance and exit of the slow-wave structure as a function of beam energy, working gas pressure, plasma density gradient along the beam, and magnetic field strength.

The microwave oscillation power at the entrance and exit of the slow-wave structure exhibited a resonance dependence on the beam electron energy. The maximum power was obtained at a beam electron energy of 18 - 19 keV, although the calculated value for the helix-plasma waveguide was 16 keV. As noted in Section 2, this discrepancy is due to the phase velocity in the helix-plasma waveguide being higher than in a plasma-free helical slow-wave structure.

Figure 2 presents the excited oscillation power, dissipated in the loads, versus the interaction zone working gas pressure for 19 keV, 9A beam at a fixed 0.15 T magnetic field. The maximum power at the slow-wave structure entrance (26 kW) and exit (40 kW) occurred at a $(2 - 4) \times 10^{-5}$ Torr pressure. The maximum summary power of 66 kW was attained at a beam power of 171 kW; thus, the electron efficiency was equal to 38%.

In order to increase the excited oscillation output power we introduced a rejection band-pass filter between the generator entrance and the matched load (5). The power generated at the system entrance and exit as a function of working gas pressure is shown in Fig. 3.

It is seen that the power absorbed in load (5) was low and independent of the gas pressure in the system. At the same time, the power dissipated in the output load (9) increased with pressure and reached 70 kW at 10^{-4} Torr. The beam energy, beam current, and magnetic field were 19 keV, 9.5 A, and 0.2 T, respectively. The electron efficiency remained the same (38%).

We recorded the frequency spectrum of generated oscillations with a wavemeter (12), integrator (14), and recorder (15). The oscillation spectrum bandwidth at the 0.1 level was 100-150 MHz in the decimeter wavelength band.

In addition, the realization of excited oscillations was recorded with a fast oscilloscope (2) to determine its autocorrelation function, frequency spectrum, and phase time-dependence by means of correlation analysis techniques.

The most interesting of the tubular electron-beam BPG operating modes is the one with the microwave pulse length equal to that of the beam current pulse. It was obtained at 15 keV beam electron energy, 13 A beam current, $6 \times 10^{10} \text{ cm}^{-3}$ plasma density (6×10^{-5} Torr working gas pressure), and 0.11 T longitudinal magnetic field in the interaction zone. The microwave power in BPG feeders amounted to 80 kW; the electron efficiency was 40%.

We carried out a microwave oscillation analysis in this mode of BPG operation. Figures 4-6 present the oscillograms of a high-frequency signals (Figure 4), the **total phase of oscillations** (Figure 5), its computer calculated autocorrelation function (Figure 6 top), and the microwave oscillation power spectrum (Figure 6 bottom). The correlation time and spectrum bandwidth are correlated by the expression $\tau \Delta f = 1$; thus, short correlation times correspond to wide frequency spectra and *vice versa*. In our case $\tau_{\text{corr}} = 2.5 \text{ ns}$.

It is well known that the shorter the correlation time (and the wider the frequency spectrum of excited oscillations), the higher their degree of stochasticity. Thus, in our case, one should expect the generated oscillations to be highly stochastic.

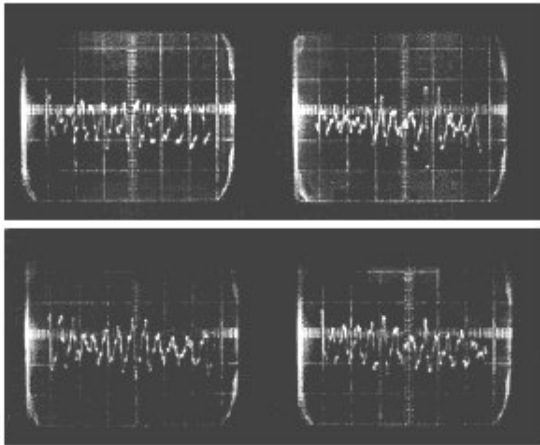


Fig. 4 – Oscillograms of a high-frequency signals

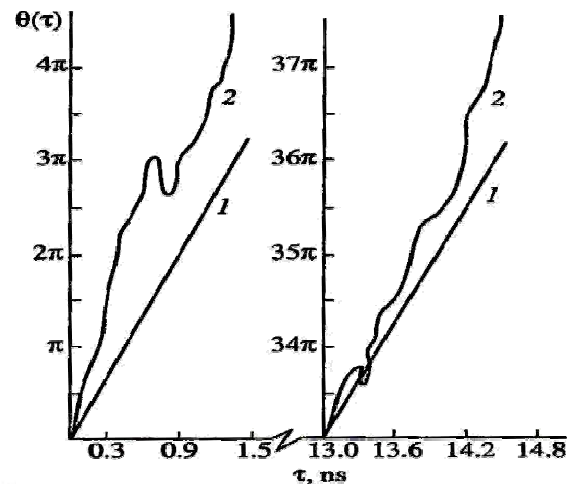


Fig. 5 – Total phase of oscillations versus time: (1) 1.2 GHz frequency regular signal; (2) oscillations excited in a plasma-beam generator at plasma density $n_p = 6 \times 10^{10} \text{ cm}^{-3}$.

Thus, there is an important conclusion to be stressed: our decimeter-wavelength microwave BPG makes it possible to control the generated oscillation stochasticity and spectrum width by varying the plasma parameters and, primarily, its density.

5. Comparison of theory with experimental results. In order to compare the theoretical results with the experimental data on the collective interaction between the electron beam and the helix-plasma waveguide waves, it is necessary, above all, to determine the beam parameters and the plasma density. In our case, the tubular beam density n_b was 10^9 cm^{-3} ; the experimentally measured plasma density was in the range of $(2 - 8) \times 10^{10} \text{ cm}^{-3}$. Due to the $\omega_b/\omega_p = 1/20$ condition, valid in our experiment, the electrons could not significantly perturb the wave field pattern notwithstanding their strong coupling to the slow-wave system. Consequently, when calculating the excited oscillation spectra, one could neglect electron beam effects within the zero approximation.

The oscillation excitation current threshold is given by formula (4). In our system $J_{th} = 3 \text{ A}$ for a calculated quality factor $Q = 45$, $f_0 = 1.3 \times 10^9 \text{ Hz}$ working frequency, and a beam Langmuir frequency depression coefficient $\mu = 0.05$.

At sufficiently high plasma densities $n_p > n_{pcr}$ bulk waves appear in this system. The beam Langmuir frequency depression coefficient for these waves is significantly higher, resulting in a corresponding threshold current decrease.

For this case, one could find from formula (4) the critical density of $6 - 8 \times 10^9 \text{ cm}^{-3}$ for a tube-shaped plasma with $(b - a) = 1 \text{ cm}$ wall thickness, this "tube" being coaxial with the electron beam.

The increase of gas pressure in the system or, with the same effect, the increase of plasma density and increase of beam current lead to the excitation of a

wide spectrum of bulk waves.

The current, corresponding to the wave spectrum broadening, was determined from formula (4) and found to be equal to $J_{cr} = 7 \text{ A}$, in fair agreement with the experimental value $J_{ecr} = 9 \text{ A}$.

6. Experimental studies mwrsjp and optical radiation

6.1. MWRSJP parameters obtained from the BPG, and the scheme of measurement of various parameters.

We study MWRSJP parameters and optical radiation characteristics from the plasma discharge of induced by MWRSJP in a gas (air for the present case), taken at low pressure. To conduct experiments, a coaxial waveguide with axial vacuum pumping is connected to the BPG. Coaxial waveguide filled with gas with impedance of about 75 ohms and a length of 1000 mm is made of brass pipes with inner diameter of 45 mm and external diameter of 50mm (see figure 7). The central conductor is a brass rod diameter of 12mm. At the ends of the coaxial waveguide, tapered flanges provide the joining of coaxial transitions. In the middle of the coaxial waveguide a tube is installed to pump gas or gas mixtures, which also mounted a thermocouple tube to monitor the pressure of the gas. Admission process of gases or gas mixtures is carried out with sufficient precision using the second inlet valve through diametrically located holes 2 mm in diameter that are situated at both ends of the coaxial waveguide. Tubes for the introduction of diagnostic probes are located along the length of the coaxial waveguide. The first tube is located at 60 mm from the input microwave power of

stochastic electromagnetic waves; the second one is placed at a distance of 260 mm and a third – at 840 mm. During the working process, such arrangement of instruments allows us to have controlled diagnostic probes of a spatial distribution, as well as to monitor parameters of the microwave discharge along throughout the waveguide length. This provides more detailed information about processes that take place inside the waveguide. To ensure the required conditions for the gas pressure, a coaxial waveguide is connected with conical coaxial 75-ohm transitions length 160 mm flange with Teflon washers 45 mm in diameter and 10 mm thick. The desired electrical contact between the

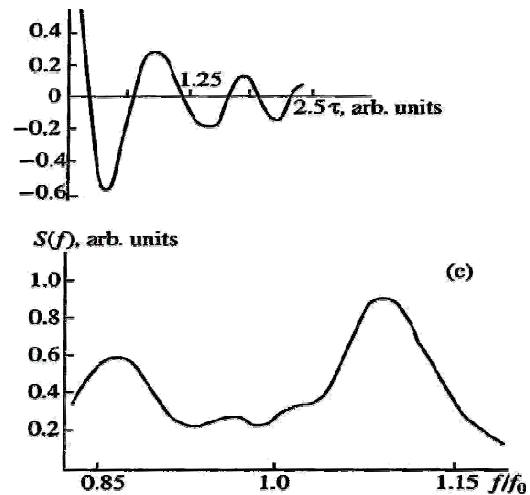


Fig. 6 – Autocorrelation function, power spectrum of oscillation realizations versus time

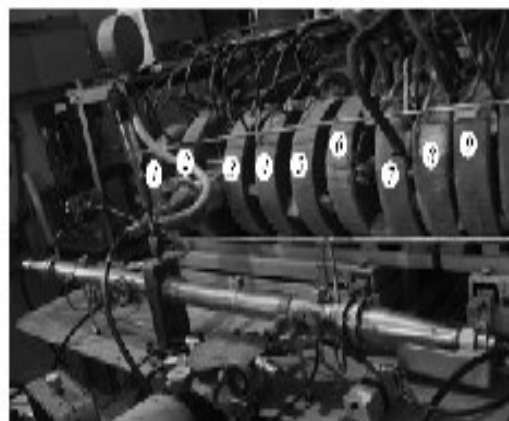


Fig. 7 – The general view of the experimental device with the coaxial waveguide

flanges of the coaxial waveguide and flanges of the conical coaxial transition provide a lead strip 3 mm thick.

The block diagram shown in figure 8 schematically represents measurements of the main parameters of the BPG and of the plasma, which is produced in the coaxial waveguide.

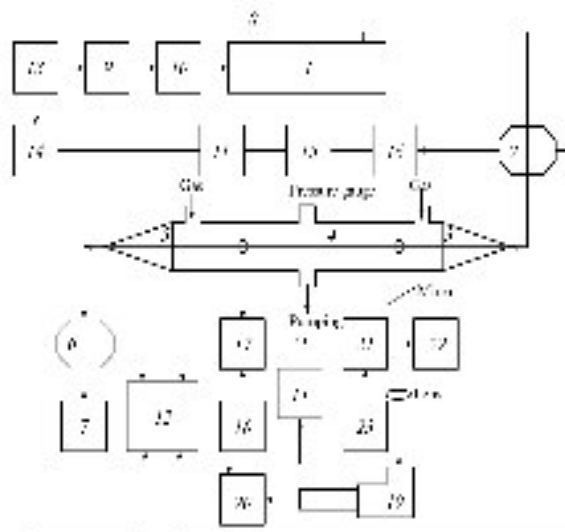


Fig. 8 – Block diagram of measurement of BPG and plasma principal parameters.

Stochastic microwave oscillations generated by the BPG (1) were supplied from the output of the slow-wave structure through a broadband directional coupler (2) and 75- Ω conical coaxial junction (3) to the input of the coaxial waveguide (4) and then, through a conical coaxial junction (5) and coupler (6), were fed to an IBM-2 high power gauge (7). For operating in the regime of narrow-band signal generation the input of the BPG slow-wave structure was attached to a shorting plug (8). The oscilloscopes (11, 12) and the submodulator (9) and modulator (10) of the high voltage supplied to the cathode of the BPG electron gun were triggered synchronously by using a timing unit (13). A time-delay circuit (14) was used to vary the instant of triggering the oscilloscopes with respect to the beginning of the high voltage pulse. This allowed us to observe the shape of the generated signal at different instants after the beginning of the electron beam pulse. A detector head (15) and D2-13 variable resistive-capacitive attenuator (16) connected to the secondary line of the coupler (2) were used to measure the envelope of microwave oscillations and the waveforms of the electron beam pulse. The temporal realizations and spectral characteristics of MWRSJP at the input and output of the coaxial waveguide were studied using an HP Agilent Infinium four-channel broadband (2.25 GHz) oscilloscope (12). A PEM-29 photomultiplier (17) powered from a VSV-2 high-voltage stabilized rectifier (18) was used to measure the integral intensity of optical radiation from the plasma. An ISP-51 three-prism glass spectrograph (19) and PEM-106 photomultiplier (20) were used for optical spectroscopy of the discharge in the coaxial waveguide.

Ignition of the discharge does not affect the penetration into dense plasma of MWRSJP what is evidenced by nearly constant amplitude at the entrance to the waveguide (curves 1 in figure 9). Because of expenditures of radiation energy on air ionization for the discharge maintenance the MWRSJP amplitude at the output of the coaxial waveguide (curves 2 in figure 9) is essentially diminished. It is also important that the MWRSJP local spectrum on the output waveguide significantly changed (curves 2' in figure 9), a peak associated with the main spectral component of MWRSJP is absent. It should be noted that in the pressure range from $P = 30$ Pa to $P = 2$ Pa at a MWRSJP power that conforming to the

optimal operating mode of BPG a similar situation is observed. The optimal operating mode of BPG corresponds to the following parameters: magnetic induction in the interaction range of the beam with slow-wave structure in BPG is $B = 0.096$ T, a high voltage is $U_{opt} = 13.2$ kV, the current electron gun is $I_{b_{opt}} = 3-5$ A, high-voltage pulse is $160 \mu\text{s}$.

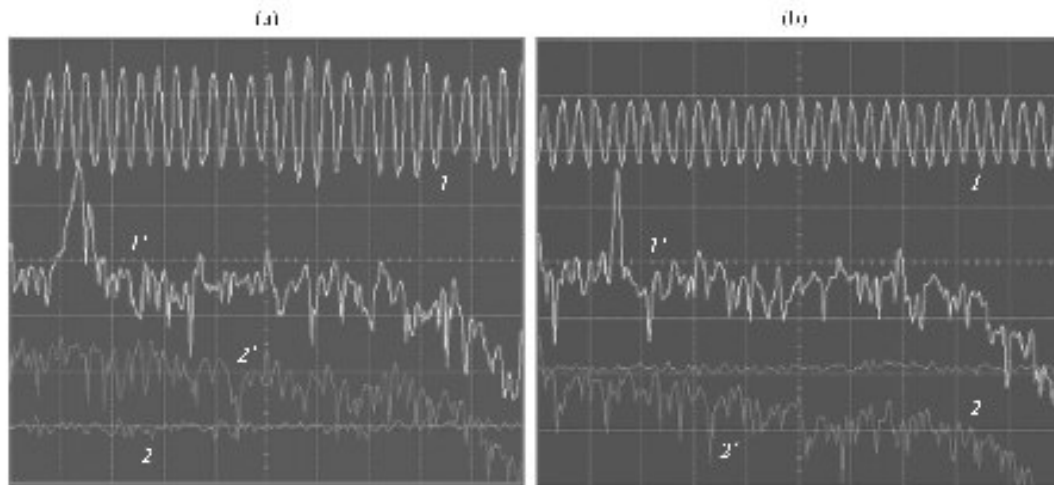


Fig. 9 – Waveforms of MWRSJP at the (1) input and (2) output of the coaxial waveguide, respectively, and local microwave spectra on a logarithmic scale (10 dB/div) at the (1') input and (2') output of the coaxial waveguide, respectively. The gas pressure in the waveguide is $P =$ (a) 2.0 and (b) 30 Pa, respectively. The time scale is 5 ns/div, and the voltage scale is $100 (\text{V cm}^{-1})/\text{div}$

Comparison of the results presented in figures 9a and 9b shows that, as the spectrum of the microwave signal used to initiate and maintain a steady-state discharge is narrowed, the amplitude of the MWRSJP electric field can be decreased by nearly a factor of 2. However, in order for the pressure range in which breakdown occurs and a steady-state discharge exists to be sufficiently broad, it is necessary that the phase jump frequency be sufficiently high (as will be seen below, it should be about one-third of the microwave frequency). Let us now analyze the measured characteristics of MWRSJP at the input and output of the coaxial waveguide in the optimal BPG mode. The oscillograms shown in figures 3,4 were processed by the method of correlation analysis, and the frequency spectra, the time dependence of the phase of microwave oscillations, and self-correlation functions were determined. Figure 4 shows the measured parameters of MWRSJP recorded at $100 \mu\text{s}$ after the beginning of the electron beam pulse in the optimal BPG mode for two air pressures corresponding to the pressure range in which discharge in air is ignited and operates stably. It can be seen that gas breakdown takes place only after the electric field amplitude of MWRSJP reaches a certain critical value, which depends on the gas pressure. The instant of discharge ignition can be easily determined from the abrupt decrease in the amplitude of the microwave signal at the output of the coaxial waveguide to almost zero. It can also be seen that the electric field amplitude required to maintain a steady-state discharge is one order of magnitude lower than that required for breakdown. From figure 9 it can be seen that, MWRSJP amplitude at the waveguide outlet is reduced substantially (more than an order of magnitude) due to the development of the discharge; the discharge ignition and maintenance lead at the waveguide outlet to a strong damping of the spectral components, which are corresponded to the maximum range of input signal into the waveguide.

Let us now consider the conditions for breakdown in air by microwave radiation from the BPG described in [13]. In optimal regime at narrowband signal of this generator the

working frequency is 500 MHz, the mean rate of the phase jumps being $\nu_{jp} = 2 \times 10^8 \text{ s}^{-1}$. It is important to keep in mind that, when the electron energy increases from zero to the ionization energy *lair*, the cross section for elastic collisions of electrons with air atoms and molecules varies greatly (by a factor of about 30), being at its maximum several times larger than the ionization cross section corresponding to electron energies of 15...20 eV. This makes it possible to initiate discharges in air by microwaves with a stochastically jumping phase at pressures as low as 4 Pa. In this case, the mean rate of phase jumps is equal to the maximum inelastic collision frequency, which corresponds to electron energies close to the ionization energy. Operation under such conditions is advantageous in that, first, no energy is lost in elastic collisions, and, second, due to the jumps in the phase, the electron diffusion remains insignificant and the electromagnetic energy is efficiently transferred to electrons.

To determine the dependence of the threshold power, required for ignition of the discharge in a coaxial waveguide, on the pressure of working gas, BPG has worked in the mode of generating the maximum output power level of narrow-band signal in which the generation of microwave radiation with a maximum frequency of phase jumps occurs. In this case part of the power with the help of a broadband directional coupler with variable coupling (see figure 10) was supplied to analyzed gas-filled coaxial waveguide.

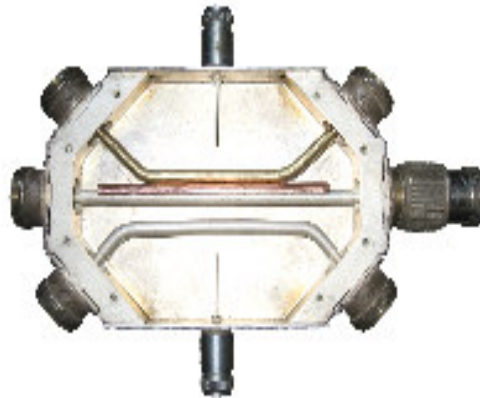


Fig. 10 – The general view of the coupler (6) internal structure

The rest of the power assigned to the matched load. Such a method of regulating the power delivered to the coaxial waveguide for ignition of the discharge allows conserving the permanent parameters of microwave radiation. In particular, this concerns the mean rate of the phase jumps and the energy spectrum density of MWRSJP, because in this situation BPG works in the same mode.

The optimal operating mode of BPG corresponds to the following parameters: magnetic induction in the interaction range of the beam with slow-wave structure in BPG is $B = 0.096 \text{ T}$, a high voltage is $U_{opt} = 13.2 \text{ kV}$, the current electron gun is $I_{b_{opt}} = 5 \text{ A}$, a high-voltage pulse is $160 \mu\text{s}$, MWRSJP peak power is $W = 36 \text{ kW}$, the pulse repetition frequency is 5 Hz . In figure 5 the general view of the coupler (6) internal structure is shown.

While conducting experiments, to determine the dependence of the threshold power on the gas pressure, the left center coax transition coupler was connected to BPG, the lower left coax transition joined the coaxial waveguide, the right central and the lower coaxial transitions were connected to the load. By changing the bond between the central and the lower shoulders of the coupler through the use of different linked curved shoulders, we adjusted the peak power coming into the coaxial waveguide from 6 kW to 28 kW.

Fig. 11 shows the dependence of peak power required for the discharge ignition in the air that filled coaxial waveguide on its pressure.

From figure 11 (curves 1, 2) it can be seen that, the peak power levels from 6 kW to 28 kW MWRSJP discharge is ignited stably at a pressure of gas (air) ranging from 1.5 Pa to 3990 Pa. This result clearly demonstrates the advantages of the discharge, supported by microwave with stochastic jumps in the phase compared with the microwave discharge in the fields of regular waves.

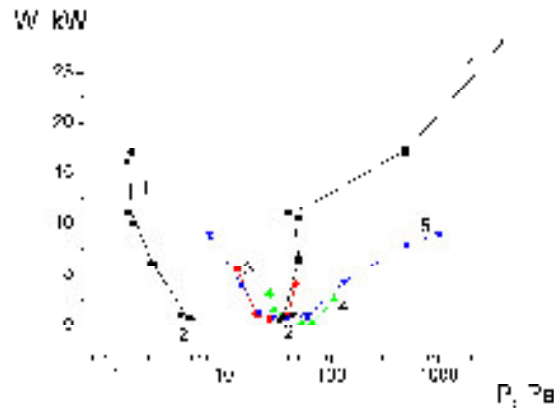


Fig. 11 – Dependences for breakdown power of a microwave signals with a stochastically jumping phase versus a pressure for air in the optimal BPG mode (curves 1 – ■, 2 - *), in the non-optimal BPG mode: for air (curve 3 - ●), argon (curve 4 – ▲), helium (curve 5 – ▼), respectively, at narrowband signal

Thus we have the opportunity to create a discharge at a pressure of almost two orders of magnitude lower than the pressure that is necessary for the fulfillment of the condition of minimum capacity of the discharge ignition by regular microwave radiation. Namely, (see [29]) for $v_{col} \approx \omega$ (where v_{col} is the frequency of binary collisions, as well ω is the frequency of microwave radiation), effectiveness of such a discharge is much higher because of the small contribution of energy loss on unnecessary elastic and inelastic collisions when working at low pressures. For comparison, dependence of microwave radiation power required for the discharge ignition in air (curve 3), argon (curve 4) and helium (curve 5), which are filled the coaxial waveguide, on its pressure, obtained while working in the non-optimal BPG mode is given. It is seen that the pressure range in which it is possible the ignition of the discharge is much narrower than under the optimal BPG mode functioning. This is due to a significant difference in mean rates of the phase jumps in these modes of BPG.

Using the delay device (14), the time for start of the oscilloscope can be modified within the length of high-voltage pulse. This circumstance allows us to observe the shape of the generated signal at a different time moments starting from the very begin of the electron beam current pulse. Features MWRSJP at the inlet and outlet of the coaxial waveguide are studied using the four-channel broadband (2.25 GHz) oscilloscope (12) HP Agilent Infinium Oscilloscope.

In the next part we present the results of experimental studies of optical characteristics of plasma discharge. Preliminary results of an optical characteristic studies presented in [30].

6.2. Experimental studies of optical radiation from the plasma discharge initiated by MWRSJP

Optical characteristics of plasma discharge initiated by MWRSJP in coaxial waveguide are examined in the conditions of BPG operation in the optimal mode in air for a wide pressure range, in which the discharge is ignited and maintained stably. For experimental studies of the integral intensity of the plasma radiation in the visible spectrum, used photoelectron multiplier (17) of type PEM-29 is attached to a high-stabilized rectifier

(18) VSV-2. For spectroscopic studies of the discharge in the visible spectrum a three-prism glass spectrograph (19) ISP-51 is used. With help of the lens, the radiation from the discharge is focused onto the entrance slit (slit width is 0.01 mm) of the spectrograph. By the output gap with width of 0.015 mm the spectrograph is attached to the photoelectron multiplier (20) of type PEM-106. The spectral sensitivity in the wavelength range from 360 nm to 700 nm of the photomultiplier PEM-106 used in experimental studies is shown in figure 12.

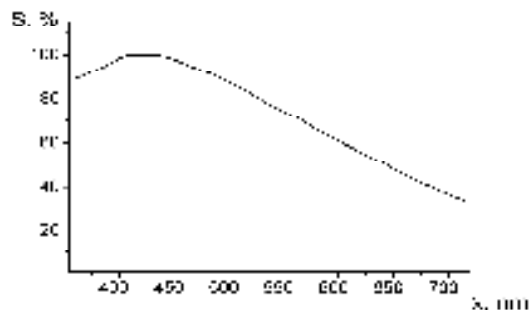


Fig. 12 – The dependence of spectral sensitivity of the photomultiplier PEM-106 versus the wavelength

From figure 12 it can be seen, that the photomultiplier PEM-106 has high sensitivity in the wavelength range from 350 nm to 550 nm. Within zone from 550 nm to 1000 nm the sensitivity is less that will lead to distortion of the discharge optical spectra which are observed on oscilloscope (11). This fact should be taken into account when the wave forms of the emission spectra are analyzed. The signal from the photomultiplier PEM-106 was fed to the digital (2 GB/s) oscilloscope (11) Le Croy Wave Jet 324 with a frequency band of 200 MHz. The ISP-51 spectrograph was calibrated using the spectral lines of a PRK-2M mercury lamp (21) and the Balmer hydrogen lines emitted by a Geissler tube (22). The mercury lamp and the Geissler tube were powered from an OU-1 lighting unit (23).

The MWRSJP power was input via the conical coaxial junction in the waveguide pumped out to a pressure of 1.33 Pa. In certain ranges of the gas pressure, gas composition, and microwave power, a discharge was ignited in the coaxial waveguide. Figure 13 shows the emission spectrum of the mercury lamp of type PRK-2M.

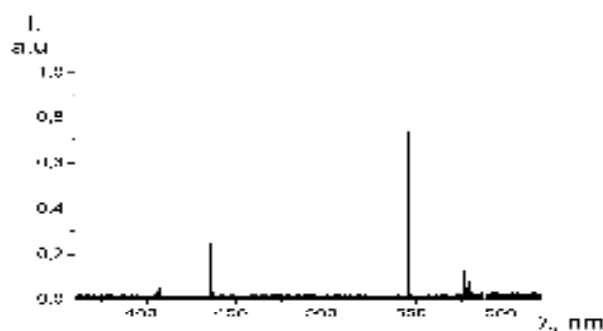


Fig. 13 – The emission spectrum of mercury lamp type PRK-2M

Remark, that in figure 13 and in the consequent figures 14-19, which presents radiation spectra from the low-pressure discharge, the real dependence of the spectral sensitivity of the photomultiplier is taken into account, and for the simplicity of comparison the same arbitrary units are used.

Figure 14 shows the photo of glow discharge at a pressure of working gas (air) of 13.3 Pa in the waveguide made through a curved quartz optical window. For the necessary observations, apertures were drilled with a diameter 2.5 mm on the lateral surface of the

coaxial waveguide in the area of the windows. On the one hand, these apertures provide properly output of the light radiation from a coaxial waveguide and, on the other hand, they prevent output of the microwave radiation from the discharge region.

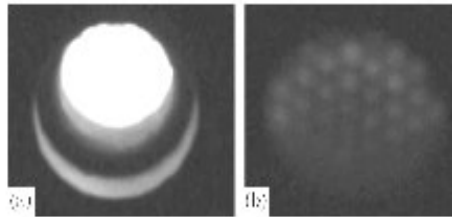


Fig. 14 – Photographs of the discharge glow in the coaxial waveguide, taken at the distances of (a) 60 and (b) 600 mm from the microwave power input in the waveguide

From figure 14 one can see, that the glow discharge intensity significantly decreases with distance from the MWRSJP input to the waveguide (for example, compare (a) and (b)). Figure 14 shows photographs of the discharge glow in the coaxial waveguide at a working gas (air) pressure of 13.3 Pa. It can be seen from figure 14 that the discharge glow is inhomogeneous over the cross section and has a filamentary structure. This is because 2.5-mm-diameter holes were made in the side wall of the coaxial waveguide near the diagnostic windows. These holes, on the one hand, provide output of optical radiation from the coaxial waveguide and, on the other hand, prevent escape of microwave radiation from the discharge region. It is seen that the discharge radiation intensity decreases along the waveguide. It should be noted that the discharge color depends on the working gas pressure and the microwave power input in the waveguide.

In Fig. 15-17 the dependence of optical radiation from the discharge on air pressure is compared at the conditions when a stable combustion of the gas discharge is held at the MWRSJP power that correspond the optimal BPG mode.

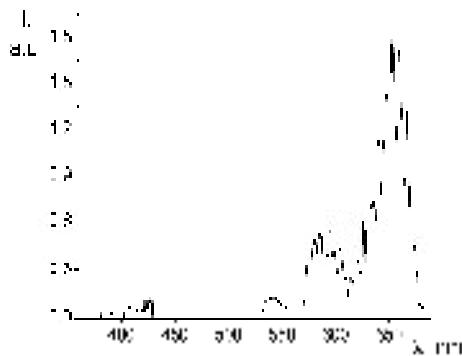


Fig. 15 - The emission spectra of discharges in air at a pressure $P = 28$ Pa

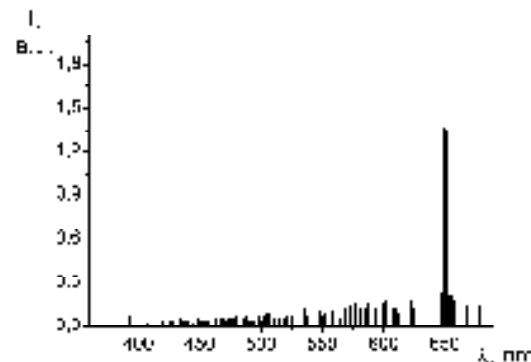


Fig. 16 - The emission spectra of discharges in air at a pressure $P = 4.8$ Pa

Figs. 15-17 show that the spectrum of optical radiation from the discharge depends strongly on the pressure of the working gas (air) in a coaxial waveguide. In particular, within the lower range of air pressure, the optical radiation from the discharge is pronouncedly enriched with shorter wavelengths.

In this way, if value of pressure is $P_1 = 28$ Pa then spectrum is depleted at the wavelengths shorter than 550 nm, i.e. red radiation prevails, see figure 15. At the same time, when the pressure is reduced nearly an order of magnitude, see figures 16, 17 a spectrum becomes significantly enriched with short wavelengths, i.e. blue light prevails. Further figures 18 and 19 represent the experimental studies of the temporal characteristics of optical radiation for two specific wavelengths within the duration of the single high-voltage pulse (160 μ s).

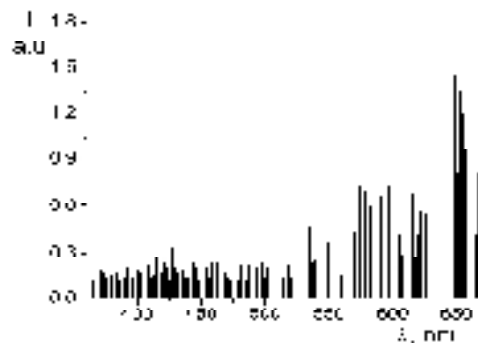


Fig. 17 - The emission spectra of discharges in air at $P = 4$ Pa

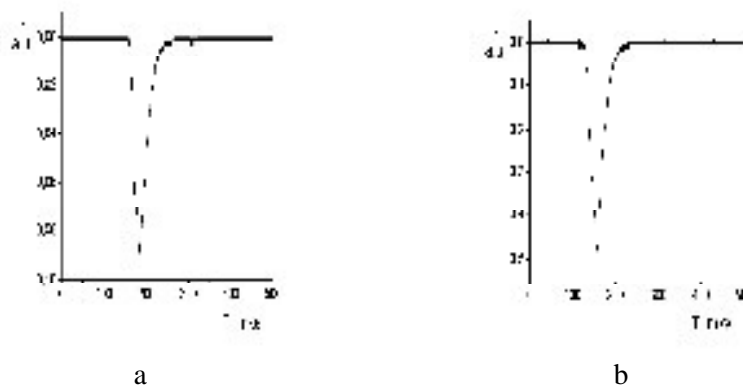


Fig. 18 – Dependence of the optical radiation intensity on time for the wavelength 485 nm within a duration of one high-voltage pulse for gas pressures of $P =$ (a) 28 and (b) 4.8 Pa

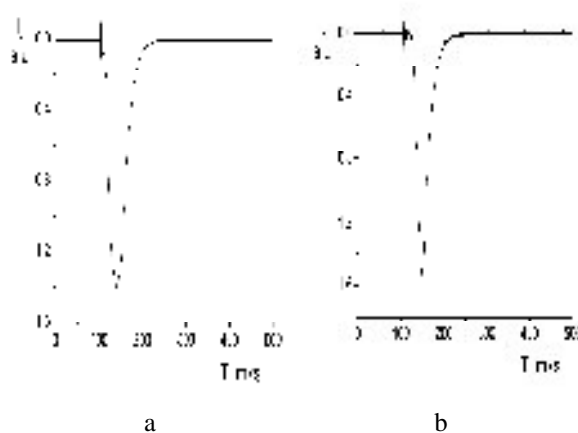


Fig. 19 – The dependence of the optical radiation intensity on time for a wavelength of 651 nm within a duration of one high-voltage pulse for gas pressures of $P =$ (a) 28 and (b) 4.8 Pa.

One can observe that the optical emission starts with a delay relatively to the beginning of current pulse (current pulse is marked on figures 18, 19 by vertical risk). However, duration of the optical emission exceeds the duration of the high voltage pulse.

Thus, relying on the quantitative indicators of the electric field intensity, frequency MWRSJP and frequency of phase jumps, etc., the prospect of creating a source of light radiation of low power (100 W) is implemented. It is based on the consideration of a stochastic microwave discharge with high efficiency at low pressure of working gas.

7. Conclusions. In this article we described the investigation of BPGs producing stochastic oscillations caused by electron beam-plasma collective interactions.

Laboratory models of high-power stochastic oscillation generators were implemented

using the slow-wave helix-plasma systems with either single or double modified helices. Their performance was investigated.

The obtained experimental results (the dispersion properties of helix-plasma waveguides, the frequency spectrum broadening mechanisms, the threshold and critical currents) turned out to be in qualitative agreement with theory.

At the stage of discharge in the coaxial waveguide, the discharge becomes nonuniform along its length due to the strong absorption of MWRSJP. The electric field amplitude decreases by more than one order when approaching to the waveguide exit.

During the [maintenance](#) of MWRSJP discharge in the waveguide, gas ionization leads to almost complete decay in the spectrum of the output signal from the coaxial waveguide of the main spectral components of the input microwave signal.

With the distance increasing from the input of MWRSJP into the coaxial waveguide, the discharge optical radiation intensity decreases significantly, becoming inhomogeneous, as well as its cross-section decreases.

With air pressure decreasing, the optical radiation from the discharge becomes more reach with shorter wavelength. Thus, if at the pressure of 20 Pa, the radiation has red colour, then at pressure of 2Pa the radiation becomes blue.

MWRSJP and discharge optical radiation are observed in time almost throughout the pulse duration of electron beam current in BPG.

When the frequency of MWRSJP signal and the frequency of phase jumps are those as observed in the conducted investigations, there is enough to have the magnitude of electric field equals to 50 V / cm, for the creation and maintenance of the discharge in air.

Thus, based on the quantitative indicators, such as the electric field intensity, frequencies of MWRSJP and phase jumps it can be expected the following. The prospective creation of an efficient light radiation source of low power (100 W) in a wide range of air pressure, in which the discharge is ignited and maintained stably, becomes a reality. The main task of future experimental and theoretical research is to optimize the gas mixture for the discharge of quasi-solar optical spectrum.

The results might also be of some use in connection with additional plasma heating in nuclear fusion devices due the fact that, the electron heating by microwave radiation with jumping phase is collisionless. Thus the heating efficiency by MWRSJP does not decrease when the temperature increases, whereas the usual heating by the regular radiation is to be collisional and becomes less and less efficient at increasing temperature. Moreover, instead of pulse working regime of BPG, the constant working regime which is important for tokamak plasma, in principle may be elaborated.

The developing of a new type of the high efficiency sources of optical radiation with quasi solar spectrum would make a fundamental breakthrough in lighting technology.

References

1. Akhiezer A.I. and Fainberg Ya.B. Beam Instability, *Otchet khFTI AN USSR* (Report of Kharkov Physics and Technology Institute, Academy of Science, USSR). 1948. P. 30.
2. Akhiezer A.I. and Fainberg Ya.B. About Interaction of beams of charged particles with electron plasma. //Dokl. Akad. Nauk SSSR. 1949. Vol. 69, no. 4. P. 555-556.
3. Akhiezer A.I. and Fainberg Ya.B. About high-frequency of electron plasmas. //Zh. Eksp. Teor. Fiz. 1951. vol. 21. P. 1262-1269.
4. Fainberg Ya.B. Interaction of beams of charged particles with plasma. //At. Energ. 1961. Vol. 11, no. 4. P. 313-315.
5. Fainberg Ya.B. Interaction of beams of charged particles with plasma. *A Survey of Phenomena in Ionized Gases*, Vienna: IAEA. 1968. P. 149-172.
6. Berezin A.K., Fainberg Ya.B., Bolotin L.I. et al. About beam instability control. *Plasma Phys. and Controll.* //Nucl. Fusion Res. Vienna: IAEA, 1969. Vol. 2. P. 723-732.
7. Berezin A.K., Fainberg Ya.B., and Bez"yazychnyi I.A. Experimental studies of possibility of instability control with help modulation. //Pis'ma Zh. Eksp. Teor. Fiz. 1968. #. 7. P. 156-160.

8. Longinov A V and Stepanov K N *High-Frequency Plasma Heating / Ed. A.G. Litvak.* (New York: American Institute of Physics) 1992. P. **93-238**
9. Parail V, Belo P, Boerner P, Bonnin X, Corrigan G, Coster D, Ferreira J, Foster A., Garzotti L., Hogewij G M D, Houlberg W, Imbeaux F, Johner J, Kochl F, Kotov V, Lauro-Taroni L, Litaudon X, Lonroth J, Pereverzev G, Peysson Y, Saibene G, Sartori R, Schneider M, Sips G, Strand P, Tardini G, Valovic M, Wiesen S, Wischmeier M, Zagorski R, JET EFDA contributors and EU ITM Integrated modelling of ITER reference scenarios // *Nuclear Fusion.* 2009. Vol. **49.** **075030**
10. Lin Y, Rice J E, Wukitch S J, Greenwald M J, Hubbard A E, Ince-Cushman A, Lin E S, Marmor L, Porkolab M., Reinke M L, Tsujii N, Wright J C, and Alcator C-Mod Team Observation of ion cyclotron range of frequencies mode conversion plasma flow drive on Alcator C-Mod // *Physics of Plasmas.* 2009. Vol. **16** **056102**
11. A E, Hughes J, Ma Y, Podpaly Y, Rice J E, Wallace G, Wilson J R, Wolfe S M, and Alcator C-Mod Group Full wave effects on the lower hybrid wave spectrum and driven current profile in tokamak plasmas. // *Phys. Plasma.* 2011. Vol. **18** **080705**
12. Daughton William 2010 Formation and Inter-action of Flux Ropes in 3D Collisionless Magnetic Reconnection *Proc. 52th APS-DPP Meeting (Chicago, IL,USA)*, invited report <http://meetings.aps.org/link/BAPS.2010.DPP.UI2.1>
13. Malova Kh V, Zelenyi L M, Mingalev O V, Mingalev I V, Popov V Yu, Artemyev A V and Petrukovich A A Current Sheet in a Non-Maxwellian Collisionless Plasma: Self-Consistent Theory, Simulation and Comparison with Spacecraft Observations. // *Plasma Physics Reports.* 2010. Vol. **36.** P. **841-858**
14. Uhm H S, Hong Y C, and Shin D H A microwave plasma torch and its applications. // *Plasma Sources Sci. Technol.* 2006. Vol. **15** P. **S26-S34**
15. Gritsinin S I, Davydov A M, Kossyi I A, Arapov K A and Chapkevich A A. A Biresonant Plasma Source Based on a Gapped Linear Micro-wave Vibrator. // *Plasma Phys. Rep.* 2011. Vol. **37** P. **263-272**
16. Dolan J T, Ury M G and MacLellan D A Microwave Powered Electrodeless Light Source *Proc. VI Int. Symp. on Science and Technology of Light Sources (Budapest, Hungary).* 1992. P. 301-311.
17. Didenko A, Zverev B, Koljashkin A and Prokopenko A. Development of Microwave Powered Electrodeless Light Source in MEPhi *Proc. of IV Int. Workshop "Microwave Discharges: Fundamentals and Applications" (Zvenigorod, Russia) /ed. by Yu.A. Lebedev. (M.: Yanus-K).* 2001. P. 235-244
18. Berezin A K, Fainberg Ya B, Artamoshkin A M, Bez'yazychny I A, Kurilko V I, Lyapkalo Yu M and Us V S Beam-Plasma Generator of Stochastic Oscillations of Decimeter Wavelength Band. // *Plasma Phys. Rep.* 1994. Vol. **20.** P. **703-709**
19. Karas' V. I. and Levchenko V. D. Penetration of a Microwave with a Stochastic Jumping Phase (MSJP) into Overdense Plasmas and Electron Collisionless Heating by It // *Problems of Atomic Sci. and Technol. Ser. Plasma Electronics and New Acceleration Methods* 2003. Vol. **4(3)**, P. **133-136**
20. Alisov A F, Artamoshkin A M, Zagrebelny I A, Zemlyansky N M, Karas' V I, Fainberg Ya B, Solodovchenko S I and Shtan' AF Experimental Study of a Propagation Microwave Radiation with Stochastic Jumping Phase in Overdense Plasmas. // *Problems of Atomic Sci. and Technol. Ser. Plasma Electronics and New Acceleration Methods.* 2003. Vol. **4(3)**, P. **69-73**
21. Karas' V I, Fainberg Ya B, Alisov A F, Artamoshkin A M, Bingham R, Gavrilenko I V, Levchenko V D, Lontano M, Mirny V I, Potapenko I F, and Starostin A N Interaction of Microwave Radiation Undergoing Stochastic Phase Jumps with Plasmas or Gases // *Plasma Phys. Rep.* 2005. Vol. **31.** P. **748-760**
22. Karas' V I, Alisov A F, Artamoshkin A M, Bingham R, Mirny V I, Gavrilenko I V, Zagrebelny I A, Potapenko I F and Us V S Gas Breakdown and Initiation of a Microwave Discharge in a Low Pressure Gas by Pulsed Microwave Radiation with a Stochastically Jumping Phase (I). // *Problems of Atomic Sci. and Technol. Ser. Plasma Electronics and New Acceleration Methods.* 2005. Vol. **5(5)**, P. **54-58**
23. Karas' V I, Alisov A F, Artamoshkin A M, Bingham R, Gavrilenko I V, Zagorodny A G, Zagrebelny I A, Lontano M, Mirny V I, Potapenko I F and Us V S Breakdown and Discharge in Low Pressure Gas Created by a Microwave Radiation Undergoing Stochastic Phase Jumps (II). // *Problems of Atomic Science and Technology. Ser. Plasma Physics.* 2006. Vol. **6.** P. **163-165**
24. Karas' V I, Karas' IV, Zagorodny A G, Zasenkov V I, Potapenko I F and Starostin A N Microwave Radiation with a Stochastically Jumping Phase in Plasmas // *Electromagnetic waves and electron systems.* 2010. Vol. **15.** P. **47-68**
25. Karas' V I, Alisov A F, Artamoshkin A M, Berdin S A, Golota V I, Yegorov A M, Zagorodny A G, Zagrebelny I A, Zasenkov V I, Karas' V I, Karas' IV, Potapenko I F and Starostin A N Low Pressure Discharge Induced by Microwave Radiation with a Stochastically Jumping Phase. // *Plasma Phys. Rep.* 2010 Vol. **36.** P. **736-749**
26. Karas' V I, Alisov A F, Artamoshkin A M, Berdin S A, Golota V I, Yegorov A M, Zagorodny A G, Zagrebelny I A, Zasenkov V I, Karas' V I, Karas' IV, Potapenko I F and Starostin A N Low Pressure Discharge

Induced by Microwave Radiation with a Stochastically Jumping Phase. //Dopovidi NAS of Ukraine. 2010. Vol. 8. P. 74-82

27. Bezyazychny I.A., Berezin A.K., Fainberg Ya.B. et al. Intensive high-frequency oscillations in beam-plasma discharge. //At. Energ. 1969. Vol. 26, #3. P. 256-259.

28. Berezin A.K., Fainberg Ya.B., and Bolotin L.I. et al. Control of beam instabilities. //Nuclear Fusion, 1969. Special suppl. P. 251-255.

[29] Raiser Yu P 1980 *Fundamentals of Modern Gas-Discharge Physics* (Moscow: Nauka, 1980)

29. Artamoshkin A M, Alisov A F, Bolotov O V, Golota V I, Karas` V I, Karas` I V, Potapenko I F, Yegorov A M and Zagrebelny I A Low pressure discharge induced by microwave with stochastically jumping phase *Proc. Int. Conf. on Plasma Physics EPC ICPP 2012*

МИКРОВОЛНОВОЕ ИЗЛУЧЕНИЕ СО СТАТИСТИЧЕСКИ ПРЫГАЮЩЕЙ ФАЗОЙ: ГЕНЕРАЦИЯ И ПРИМЕНЕНИЕ ДЛЯ РАЗВИТИЯ НОВОГО ТИПА ИСТОЧНИКОВ ОПТИЧЕСКОГО ИЗЛУЧЕНИЯ

В. И. Карась, В. И. Голота, А. М. Егоров, И. Ф. Потапенко, А. Г. Загородний

Приведены результаты теоретических и экспериментальных исследований по генерации стохастических колебаний в дециметровом диапазоне длин волн, в связи с коллективным взаимодействием электронного пучка с плазмой. Возможность создания пучково-плазменных генераторов стохастических колебаний, работающих в квазинепрерывном режиме продемонстрирована. Описаны методы исследования и изучены основные характеристики генерируемых колебаний. Исследован плазменный разряд, инициированный микроволновым излучением со стохастическими скачками фазы (МВИССФ) в коаксиальном волноводе в оптимальном режиме работы плазменно-пучкового генератора. В этой статье найдены: условия зажигания СВЧ-разряда, его стабильное поддержание в воздухе МВИССФ, диапазон давлений, в котором требуемая мощность минимальна. Экспериментально исследованы оптические характеристики плазмы разряда в широком диапазоне давлений воздуха. В целом исследование направлено на разработку новых типов источников оптического излучения.

МІКРОХВИЛЬОВЕ ВИПРОМІНЮВАННЯ ЗІ СТОХАСТИЧНО СТРИБКОВОЮ ФАЗОЮ: ГЕНЕРАЦІЯ ТА ЗАСТОСУВАННЯ ДЛЯ РОЗВИТКУ НОВОГО ТИПУ ДЖЕРЕЛ ОПТИЧНОГО ВИПРОМІНЮВАННЯ

В. І. Карась, В. І. Голота, О. М. Єгоров, І. Ф. Потапенко, А. Г. Загородній

Наведено результати теоретичних та експериментальних досліджень по генерації стохастичних коливань в дециметровому діапазоні довжин хвиль, у зв'язку з колективною взаємодією електронного пучка з плазмою. Можливість створення пучка плазмових генераторів стохастичних коливань, що працюють в квазинеперервному режимі продемонстровано. Описані методи дослідження і вивчені основні характеристики генерованих коливань. Досліджений плазмовий розряд, який ініційовано мікрохвильовим випромінюванням зі стохастично стрибковою фазою (МХВССФ) в коаксіальному хвилеводі в оптимальному режимі оперування плазмово-пучкового генератора. У цій статті знайдено умови запалювання НВЧ розряду, його стабільного підтримання в повітрі МХВССФ, діапазон тиску, при якому необхідна потужність мінімальна. Експериментально досліджено оптичні характеристики плазми розряду в широкому діапазоні тисків повітря. В цілому дослідження спрямоване на розробку нових типів джерел оптичного випромінювання.